CAMBRIDGE
UNIVERSITY PRESS

Article

Saccoite, $Ca_2Mn_2^{+3}F(OH)_8 \cdot 0.5(SO_4)$, a new, microporous mineral from the Kalahari Manganese Field, South Africa

Gerald Giester[1]* , Christian L. Lengauer[1], Chutimun Chanmuang N.[1], Dan Topa[2], Jens Gutzmer[3] and Karl-Ludwig von Bezing[4]

[1]Institut für Mineralogie und Kristallographie, Universität Wien - Geozentrum, Josef-Holaubek-Platz 2, 1090 Wien, Austria; [2]Naturhistorisches Museum Wien, Burgring 7, 1010 Vienna, Austria; [3]Helmholtz-Zentrum Dresden-Rossendorf, Helmholtz Institute Freiberg for Resource Technology, Chemnitzer Str. 40, 09599 Freiberg, Germany and [4]Independent Researcher, Kimberley 8301, RSA

Abstract

Saccoite, $Ca_2Mn_2^{3+}F(OH)_8 \cdot 0.5(SO_4)$, is a new mineral found at the N'Chwaning III mine, Kalahari Manganese Field, Northern Cape Province, Republic of South Africa. It occurs as fillings of voids in hydrothermally altered manganese ore (comprising mostly of bixbyite and baryte). Further associated minor minerals are braunite, gypsum, chlorite, sturmanite and ettringite. Saccoite forms small needles, felted crystal masses or crusts. The new mineral is olive green, transparent, with white streak and vitreous lustre. No luminescence is observed. Saccoite is uniaxial (–) with refractive indices at 589(1) nm of $\omega = 1.705(5)$ and $\varepsilon = 1.684(2)$. Pleochroism is distinct, i.e. bluish green (ω) and yellowish green (ε). The chemical composition was studied by means of an electron probe micro-analyser (EPMA) using wavelength-dispersive X-ray spectrometry (WDS). The empirical mineral formula is $Ca_{2.06}Mn_{1.78}^{3+}Cu_{0.10}Mg_{0.07}F_{0.97}(OH)_{8.02}(SO_4)_{0.39}$. The unit-cell dimensions of saccoite (space group $P4/ncc$) are $a = 12.834(3)$ Å, $c = 5.622(2)$ Å, $V = 926.0(4)$ Å^3, and the calculated mass density is 2.73 g·cm^{-3}. Saccoite exhibits a heteropolyhedral framework structure that is composed of edge- and corner sharing $CaF_2(OH)_6$ and $M(OH)_6$ polyhedra ($M = Mn^{3+}$ and Cu^{2+}) with large channels along [001], which host disordered and only partially occupied groups, especially SO_4^{2-}. The hydrogen atoms of the OH groups point into the channel to form hydrogen bonds with the channel anions. Ca–F distances are ~2.3 Å, the Ca–OH distances in the range of 2.44–2.58 Å, and the $M(OH)_6$ octahedron is strongly 4+2 Jahn-Teller distorted ($4 \times$ ~1.92 Å, 2×2.27 Å). The F atom is tetrahedrally coordinated to calcium atoms. The strongest lines in the powder X-ray diffraction pattern [d in Å (relative intensity) (hkl)] are: 9.0735 (35) (110), 4.5370 (95) (220), 4.0644 (20) (310), 3.0105 (100) (321), 2.8117 (20) (002), 2.7242 (75) (411), 1.9755 (35) (611), and 1.8142 (20) (550).

Introduction

One of the authors (K-L. v.B.) first noticed the new mineral in 2009 as tiny green spots on a few specimens offered by mineral dealer Donny Riekert (deceased) in the town of Kuruman, Northern Cape Province, Republic of South Africa. Thorough queries revealed that the material originates from the N'Chwaning III mine of the Kalahari Manganese Field. To date, only a very limited number of saccoite specimens have been verified.

Preliminary investigations by single-crystal X-ray diffraction methods in the years 2012 to 2014 (G.G.) suggested the presence of a hitherto unknown microporous mineral, however only further examinations in 2018 allowed the full characterisation as a new species. This work is part of a long-term study on the occurrence of rare minerals described for the Kalahari Manganese Field (Giester and Rieck, 1994, 1996; Rieck *et al.*, 2015; Giester *et al.*, 2016).

Mineral name and type material

The new mineral species is named for Guido Sacco (1900–1994) and his son Desmond Sacco (born 1942). They both played a pivotal role in the exploration and development of mining in the Postmasburg and Kalahari Manganese Field of the Northern Cape Province, Republic of South Africa, including the type locality. Desmond Sacco has accepted the proposal of the name 'saccoite'. Mineral and name have been approved by the Commission on New Minerals, Nomenclature and Classification of the International Mineralogical Association under the number IMA2019-056 (Giester *et al.*, 2019). The holotype material is deposited in the mineral collection of the Natural History Museum Vienna, Austria, inventory number O1784.

Occurrence

The samples originate from the N'Chwaning III underground mine, Kalahari Manganese Field, Northern Cape Province, Republic of South Africa (27°7′50″S, 22°51′31″E). They were found in the Northwest section in the upper part of the ore body. Saccoite was noted as isolated sprays of light green needles,

*Author for correspondence: Gerald Giester, Email: gerald.giester@univie.ac.at

not longer than a millimetre in length, lining and filling minute vugs between interlocking sparry white calcite and baryte crystals in hydrothermally altered high-grade bixbyite–hematite ores. Baryte and calcite overgrow very coarse crystalline, euhedral bixbyite cubes with edge lengths reaching up to a centimetre. Locally, these bixbyite crystals are found to be covered by millimetre-sized light brown garnet crystals, most likely andradite. Further associated minerals are minor braunite, gypsum, chlorite, sturmanite and ettringite.

The coarse crystalline bixbyite–hematite assemblage is typical for so-called Wessels-type ores (Gutzmer and Beukes, 1993, 1996; Cairncross et al., 1997). These ores formed by intensive, structurally-controlled hydrothermal alteration from carbonate-rich sedimentary manganese ores of the Palaeoproterozoic Hotazel Formation (Gutzmer and Beukes, 1993). Hydrothermal fluid flow responsible for the alteration has been dated to ca. 1.01 Ga (Gnos et al., 2003) thus coinciding with the Namaqua–Natal Orogeny along the western edge of the Kalahari Craton (Cairncross et al., 1997).

Appearance, physical and optical properties

Small needles (see Fig. 1a–c) up to 1.5 mm along [001] and 10 µm in thickness are found in vugs between baryte and bixbyite crystals. Felted crystal masses to 5 mm fill small cavities. Dendritic crystals are developed occasionally on cleavage planes in baryte. Observed forms are prisms and pinacoid, no twinning but parallel intergrowth is abundant.

The mineral is brittle, neither cleavage nor preferred parting has been observed. The Mohs hardness and density could not be determined reliably due to the fragility of the needles, the calculated density is 2.73 g·cm^{-3} based on the cell volume refined from single-crystal X-ray diffraction data and empirical chemical formula.

Saccoite is transparent with pale to olive-green colour, and has white to light green streak and vitreous lustre. This colour is presumably caused by minor incorporation of Cu^{2+} into the structure. No luminescence was observed under either long-wave or short-wave ultraviolet irradiation. A single needle was mounted on a glass fibre and inspected under a Leitz Ortholux polarising microscope equipped with a Trelle micro-refractometer spindle stage using Cargille refractive index liquids (B series [n: 1.644–1.700, Δn 0.004) and M series (n: 1.71–1.80, Δn 0.01)]. The optical orientation of the indicatrix was determined by extinction curves applying the refractive index liquid ($n = 1.70$) and *EXCALIBR* software (Gunter et al., 2004). Saccoite was proven to be uniaxial (–) with a straight extinction. The refractive indices at 589(1) nm are $\omega = 1.705(5)$ and $\varepsilon = 1.684(2)$, with birefringence –0.021. The pleochroism is distinct (bluish green // ω – yellow green // ε), the dispersion is weak, with r < v. Calculation of the equilibrium constant K_c for the empirical formula using the Gladstone–Dale relationship (Gladstone and Dale, 1863) with the values given by Mandarino (1976), combined with the optical data, resulted in a compatibility index for the empirical formula of –0.005, which is rated as superior (Mandarino, 1981).

Chemical composition

Chemical analyses (11 spots) were carried out with an JEOL JXA-8500F EPMA system (WDS mode, 15 kV, 20 nA and 15 µm beam diameter). The H_2O content could not be determined directly due to the scarcity and limited mass of pure material but is derived from the structure refinement. Analytical data are given in Table 1. The empirical composition calculated on the basis of $\Sigma(Ca, Mn^{3+},$
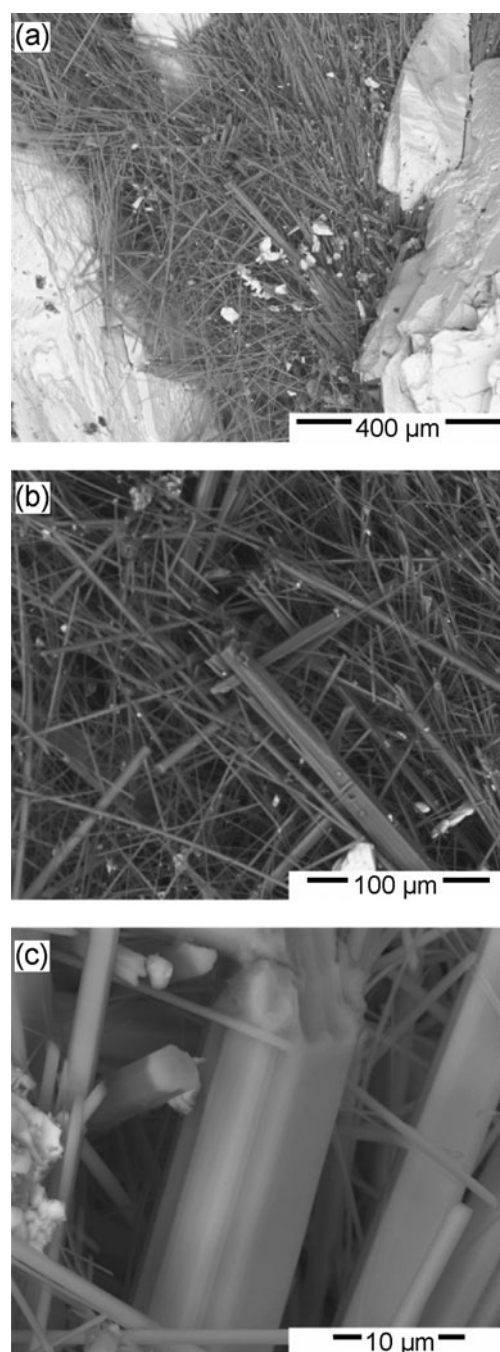

Fig. 1. Secondary electron images of saccoite needles within a void between baryte crystals. Fragment from holotype specimen.

Table 1. Chemical composition (wt.%) of saccoite.

Constituent	Mean	Range	S.D.	Standard
CaO	30.33	29.06–31.45	0.70	Wollastonite
Mn$_2$O$_3$	36.9	36.26–37.51	0.49	Tephroite
CuO	1.99	1.05–2.74	0.46	Cu metal
MgO	0.7	0.49–0.90	0.12	MgO
FeO	nd			Troilite
SO$_3$	8.21	7.11–8.91	0.50	Troilite
F	4.86	4.56–5.04	0.15	Apatite
O≡F	–2.05			
H$_2$O*	18.98			
Total	99.92	98.51–100.63	0.71	

S.D. = standard deviation (2σ uncertainty); nd = not detected.
*H$_2$O was calculated from stoichiometry.

Table 2. Powder X-ray diffraction data (*d* in Å) for saccoite.

I/I_{100}	d_{obs}	d_{calc}	h	k	l
35	**9.0735**	**9.0752**	**1**	**1**	**0**
95	**4.5370**	**4.5376**	**2**	**2**	**0**
20	**4.0644**	**4.0586**	**3**	**1**	**0**
100	**3.0105**	**3.0074**	**3**	**2**	**1**
20	**2.8117**	**2.8109**	**0**	**0**	**2**
75	**2.7242**	**2.7232**	**4**	**1**	**1**
15	2.5759	2.5747	2	0	2
10	2.3903	2.3896	2	2	2
15	2.3105	2.3108	3	1	2
5	2.2685	2.2688	4	4	0
15	2.0087	2.0081	4	2	2
35	**1.9755**	**1.9754**	**6**	**1**	**1**
5	1.8755	1.8751	5	1	2
20	**1.8142**	**1.8150**	**5**	**5**	**0**
5	1.7795	1.7798	6	4	0
5	1.7651	1.7655	4	4	2
10	1.7330	1.7330	5	3	2
10	1.6838	1.6852	7	3	0
15	1.6585	1.6582	3	2	3
5	1.5559	1.5564	8	2	0
10	1.5245	1.5248	7	1	2
10	1.4516	1.4512	8	3	1
5	1.4012	1.4011	6	1	3
5	1.3421	1.3425	2	2	4
5	1.3176	1.3178	7	5	2
10	1.2837	1.2840	7	2	3
5	1.2697	1.2695	9	4	1
5	1.2194	1.2190	9	3	2
5	1.1807	1.1804	8	7	1

Note: Bragg peaks with relative intensities ≥20% are marked in bold.

Table 3. Crystal data and details of the single-crystal intensity measurement and structure refinement for saccoite.

Crystal data	
Ideal formula	$Ca_2Mn_2^{3+}F(OH)_8 \cdot 0.5(SO_4)$
Crystal dimensions (mm^3)	0.7 × 0.05 × 0.04
Crystal system, space group	Tetragonal, *P4/ncc*
Temperature (K)	293(1)
a, *c* (Å)	12.8352(14), 5.6213(6)
V (Å^3)	926.1(2)
Z	4
Calculated density (g cm^{-3})	2.73
μ (mm^{-1})	3.95
Data collection	
Crystal description	Green needle
Instrument	Bruker APEXII-CCD
Radiation type	Mo*K*α
Number of frames	920
θ range (°)	4.49–36.58
Absorption correction	Multi-scan
T_{min}, T_{max}	0.43, 0.75
No. of meas. reflections	36,573
No. of unique and obs. [$I >2\sigma(I)$] reflections	1148, 927
R_{int}	0.075
Data completeness to 36.58°θ (%)	0.997
Indices range of *h*, *k*, *l*	$-21 \le h \le 21, -21 \le k \le 21, -9 \le l \le 9$
Refinement	
Number of parameters, restraints	49, 2
R_1 [$I >2\sigma(I)$], R_1(all)*	0.0317, 0.0425
wR_2 [$I >2\sigma(I)$], wR_2 (all)	0.0804, 0.0895
a, *b***	0.025, 2.7
GoF	1.21
$\Delta\rho_{max}$, $\Delta\rho_{min}$ (e^{--} Å^{-3})	1.73, −0.93

*$R_1 = \Sigma F_o - F_c / \Sigma F_o$; $wR_2 = [\Sigma w(F_o^2 - F_c^2)^2 / \Sigma w(F_o^2)^2]^{1/2}$.
**$w = 1 / [\sigma^2(F_o^2) + (a \times P)^2 + b \times P]$; $P = \{[\text{max of (0 or } F_o^2) + 2F_c^2\} / 3$.

$Cu,Mg) = 4$ is $Ca_{2.06}Mn_{1.78}^{3+}Cu_{0.10}Mg_{0.07}F_{0.97}(OH)_{8.02}(SO_4)_{0.39}$; simplified $Ca_2(Mn^{3+},Cu^{2+})_2F(OH)_8 \cdot 0.5(SO_4)$. The ideal formula $Ca_2Mn_2^{3+}F(OH)_8 \cdot 0.5(SO_4)$ requires CaO 28.53, Mn_2O_3 40.16, SO_3 10.18, F 4.83, O≡F −2.03, H_2O 18.33, total 100 wt.%.

The refined unit-cell parameters (Holland and Redfern, 1997) are $a = 12.834(3)$ Å, $c = 5.622(2)$ Å and $V = 926.0(4)$ Å^3, in good agreement to the ones obtained from single-crystal X-ray work. The strongest lines in the powder X-ray pattern [*d* in Å (I/I$_{100}$) (*hkl*)] are: 9.0735 (35) (110), 4.5370 (95) (220), 4.0644 (20) (310), 3.0105 (100) (321), 2.8117 (20) (002), 2.7242 (75) (411), 1.9755 (35) (611) and 1.8142 (20) (550).

Powder X-ray diffraction

Powder X-ray diffraction data (Table 2) were collected with a Gandolfi camera (114.59 mm diameter) utilising Cu*K*α radiation.

Table 4. Atom coordinates and displacement parameters (Å^2) for saccoite.

	x/a	y/b	z/c	U_{iso/eq}		
Ca	0.64949(3)	0.14949(3)	¼	0.01226(11)		
Mn*	0.54233(2)	0.45767(2)	¼	0.00997(10)		
F	¾	¼	½	0.0112(4)		
O1	0.52086(12)	0.59317(11)	0.3917(3)	0.0140(2)		
H1	0.574(2)	0.627(2)	0.414(6)	0.021		
O2	0.68134(11)	0.44496(12)	0.3723(3)	0.0148(2)		
H2	0.700(2)	0.5029(17)	0.413(6)	0.022		
S**	¾	¾	0.1680(10)	0.0511(12)		
O3**	0.7437(8)	0.6542(6)	0.432(5)	0.199(9)		

	U^{11}	U^{22}	U^{33}	U^{23}	U^{13}	U^{12}
Ca	0.01333(14)	0.01333(14)	0.0101(2)	−0.00040(12)	0.00040(12)	−0.00428(15)
Mn*	0.01043(12)	0.01043(12)	0.00906(16)	−0.00055(9)	−0.00055(9)	0.00298(11)
F	0.0116(5)	0.0116(5)	0.0104(8)	0	0	0
O1	0.0154(6)	0.0128(5)	0.0139(6)	−0.0015(5)	−0.0005(5)	0.0010(4)
H1						
O2	0.0126(6)	0.0158(6)	0.0160(6)	0.0006(5)	−0.0018(5)	0.0010(5)
H2						
S**	0.0149(5)	0.0149(5)	0.124(4)	0	0	0
O3**	0.049(4)	0.046(4)	0.50(3)	−0.025(12)	−0.014(10)	0.003(4)

*Mn = (Mn$_{0.89}$, Cu$_{0.05}$, Mg$_{0.03}$ and Ca$_{0.03}$) based on EPMA.
**The disordered atoms within the channel, S and O3, were refined with positions half occupied.

Table 5. Selected interatomic distances (*d*, Å) and bond valence strengths in valence units (vu) for saccoite.

	d, Å	vu		*d*, Å	vu
Ca–F	2.3029(4) ×2	0.58	Mn–O2	1.9190(15) ×2	1.30
Ca–O1	2.4368(16) ×2	0.56	Mn–O1	1.9327(15) ×2	1.25
Ca–O2	2.4788(16) ×2	0.50	Mn–O1	2.2671(15) ×2	0.50
Ca–O2	2.5802(15) ×2	0.38	<Mn–O>	2.04	3.06
<Ca–O,F>	2.45	2.02			
O1–H1	0.81(2)		O1···O3	2.71	
O2–H2	0.81(2)		O2···O3	2.82	

Single-crystal X-ray diffraction data and crystal-structure refinements

Needles of saccoite with homogeneous extinction, mounted on glass capillaries with laboratory grease, were selected for single-crystal X-ray data collections. The samples were studied at room temperature on a Bruker APEXII diffractometer equipped with a charge-coupled device (CCD) area detector and an Incoatec Microfocus Source IµS (30 W, multilayer mirror and Mo*K*α). Several sets of phi- and omega-scans with 1.5° scan width were collected at a crystal–detector distance of 40 mm up to 70°2θ full sphere. The absorption was corrected by the evaluation of partial multi-scans. Reflection data were processed using the Bruker *APEX3* software suite (Bruker, 2020). The crystal structure was solved by direct methods in space group *P4/ncc* and refined by full-matrix least-squares techniques with the *Shelx* software (Sheldrick, 2015, 2018). Selected crystal parameters and a summary of data collection and structure refinements are given in Table 3. Saccoite is characterised by channels along [001], which house disordered and only partially occupied groups, especially SO_4^{2-}, which could be only crudely localised. Final atom positions and important interatomic distances and angles are listed in Tables 4 and 5, respectively. The crystallographic information file has been deposited with the Principal Editor of *Mineralogical Magazine* and is available as Supplementary material (see below).

Raman spectroscopy

Raman spectra of saccoite were obtained at room temperature by mean of a dispersive Horiba LabRAM Evolution spectrometer. This system was equipped with an Olympus BX41 series optical microscope and a Peltier-cooled CCD detector. The focal length is 800 mm. A diffraction grating with 1800 grooves per mm was used to disperse the scattered light. Raman spectra were excited by a 532 nm frequency-doubled Nd:YAG laser. The laser power (measured behind the objective) was 1.2 mW. Note that preliminary tests with 12 mW laser power resulted in local sample disintegration, which is assigned to significant warming
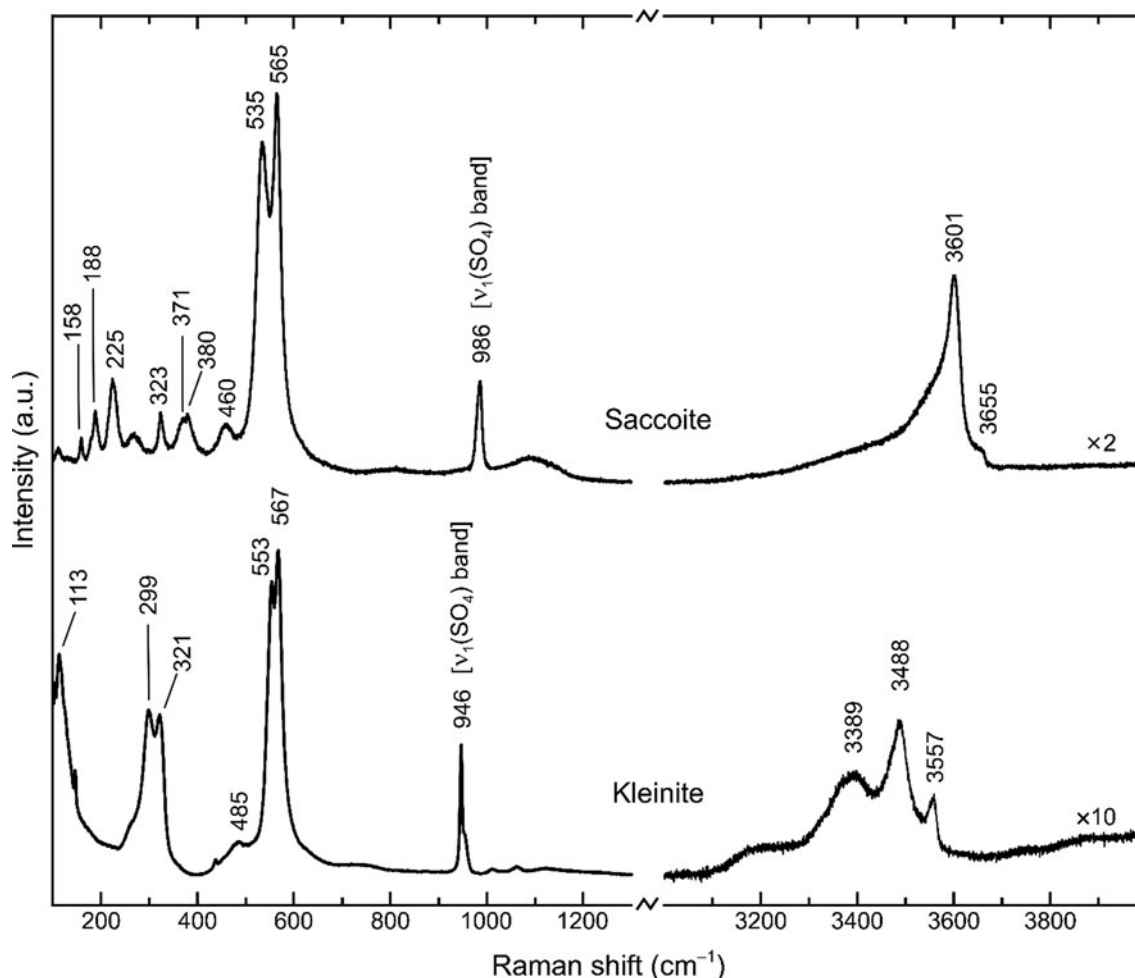
Fig. 2. Raman spectrum (532 nm excitation) of saccoite, shown in comparison with the – somehow apparently similar – spectrum of kleinite.
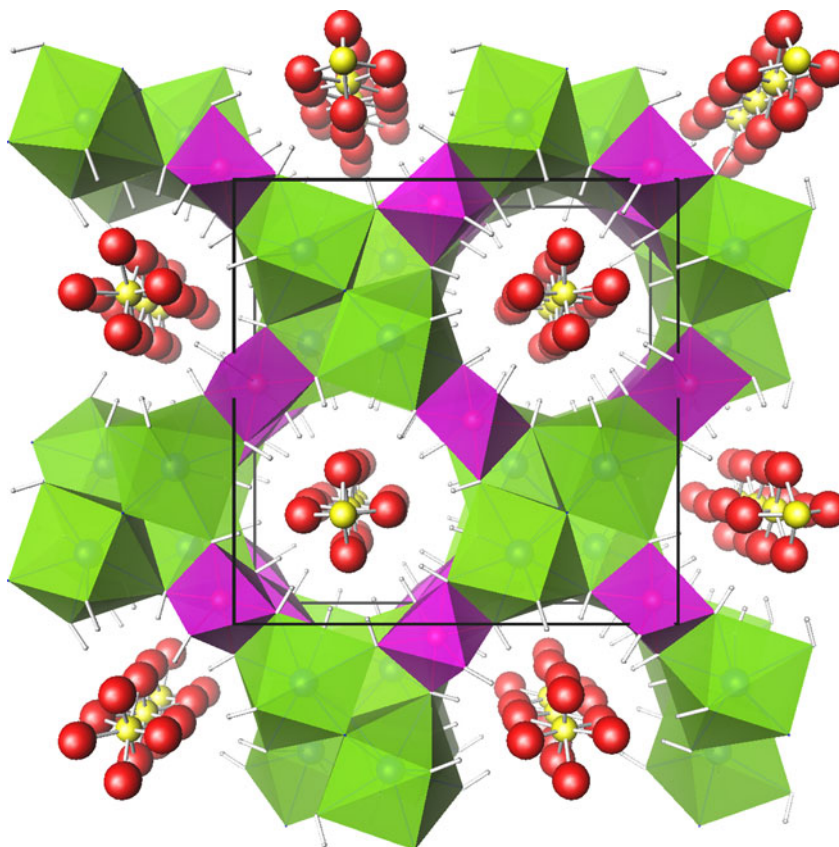
Fig. 3. Perspective view of the structure of saccoite projected along [001]. CaF$_2$(OH)$_6$ antiprisms are illustrated in green, M(OH)$_6$ octahedra in magenta and oxygen atoms of disordered sulfate groups in red. All structure drawings were done with *ATOMS* software (Dowty, 2016)

in the focal-spot area due to too intense absorption of laser light. An Olympus 50× objective (numerical aperture 0.55) was used to focus the laser beam onto the sample surface and to collect the scattered light. The spectral resolution was ∼1 cm^{-1}. Wavenumber calibration was done using the Rayleigh line and Kr-lamp emissions, resulting in a wavenumber accuracy better than 0.5 cm^{-1}. For further analytical details see Nasdala *et al.* (2018).

The Raman spectrum of saccoite is shown in Fig. 2. It is dominated by a pair of intense bands at 535 and 565 cm^{-1}, and a narrow, intense band at 986 cm^{-1}. Band assignments of the former remain unclear whereas the latter is interpreted as v_1(SO$_4$) mode (i.e. symmetric stretching vibrations of sulfate groups),

hence supporting the presence of SO$_4$ groups as derived from results of chemical analyses. The hydroxyl-stretching range shows a distinct band at 3602 cm^{-1}. This band has a shoulder at ca. 3556 cm^{-1} and clear asymmetry towards the low-energy side (3500–3600 cm^{-1}), suggesting that there exist (lower amounts of) additional, non-equivalent OH sites in the structure.

To the best of our knowledge, no related Raman spectrum exists, which seems to correspond well to the fact that there is no other mineral whose structure is related closely to that of saccoite. In database searches, however, analysts may be puzzled by the apparent similarity of the Raman spectrum of saccoite with that of kleinite, Hg$_2$N(Cl,SO$_4$)·n(H$_2$O) (Sachs, 1905; Giester *et al.*, 1996). There is no structural similarity between kleinite

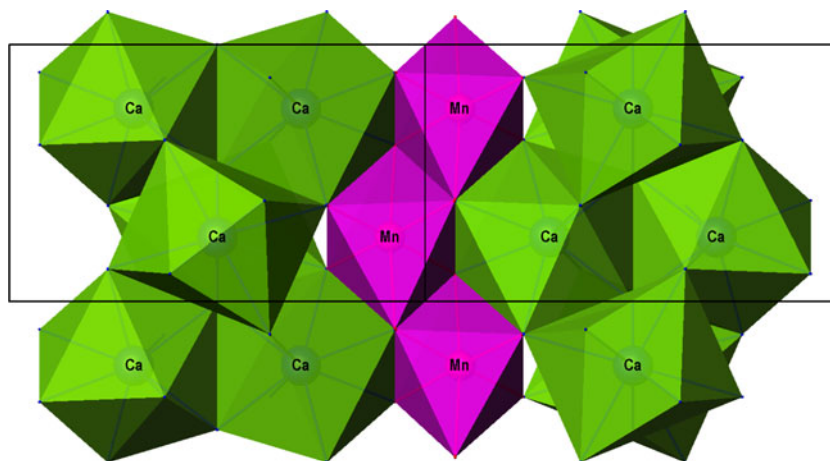**Fig. 4.** Structure detail of saccoite projected along [110]. CaF$_2$(OH)$_6$ antiprisms are illustrated in green, M(OH)$_6$ octahedra in magenta. Hydrogen atoms are omitted.
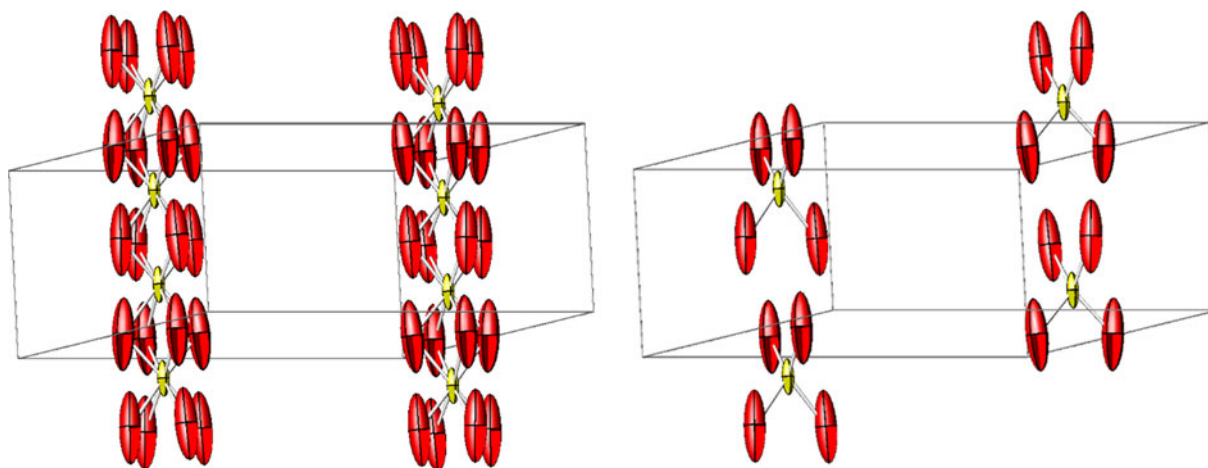
Fig. 5. Selected detail of the channel filling in saccoite. Thermal ellipsoids (50% probability) for disordered atoms of the sulfate group are shown. Left: half-occupied disordered SO_4 groups; Right: Arbitrary channel filling disregarding space group symmetry.

and saccoite, except both minerals are characterised by SO_4 groups in channels. As the Raman spectrum of kleinite has not yet been described in the literature and is only contained in databases, we provide it here as a reference in comparison with the saccoite spectrum. The reference spectrum was obtained from kleinite from the Terlingua District, Brewster Co., Texas, USA (sample #H3845 in the mineral collection of the Natural History Museum, Vienna); the identity of this sample was confirmed using single-crystal X-ray diffraction. Note that in spite of similar double bands at around 550 cm^{-1}, distinguishing the Raman spectra of saccoite and kleinite is straightforward, based on differences in their low-energy (<400 cm^{-1}) and OH-stretching ranges.

Structure description and discussion

The crystal structure of saccoite features a heteropolyhedral framework (see Fig. 3) composed of edge- and corner sharing $CaF_2(OH)_6$ and $M(OH)_6$ polyhedra ($M = Mn^{3+}$, Cu^{2+}, Mg^{2+} and Ca^{2+}) thus establishing large, eight-membered channels along [001]. The $CaF_2(OH)_6$ polyhedron can be fairly well described as a tetragonal antiprism with Ca–F distances of 2.3 Å, the Ca–OH distances are in the range of 2.44–2.58 Å. These $CaF_2(OH)_6$ antiprisms share common edges among each other, arranged in columns along [001]. The F atom, tetrahedrally coordinated to calcium ions, is the central element of these columns. The $M(OH)_6$ octahedron is strongly 4+2 Jahn-Teller distorted ($4 \times \sim 1.92$ Å, 2×2.27 Å). $M(OH)_6$ groups are linked to each other via common edges O2–O1 and O1–O1 to form zig-zag chains along [001] and further share edges with $CaF_2(OH)_6$ antiprisms (Fig. 4). A one-dimensional, non-interconnecting microporous framework results with 4.43 to 5.33 Å as a maximum diameter of a 'sphere' that can be accommodated in the channel (Foster *et al.*, 2006), estimated on the basis of (O1–O1) and (O2–O2) separation distances, respectively. Bond valence calculations (Table 5, Brese and O'Keeffe, 1991) yield bond strengths of 2.02 and 3.06 valence units (vu) for the Ca and Mn sites, respectively. The hydrogen atoms of the OH groups formed by O1 and O2 point into the channel, which houses disordered and only partially occupied molecular groups, especially SO_4^{2-}. Hydrogen bonds probably occur towards the O3 oxygen atom of the anionic groups within the channel, ranging from 2.7 to 3.0 Å.

The extra-framework content of the channel is strongly disordered and only partially occupied. Due to space group P4/ncc (number 130, origin choice 2) of the $[Ca_2Mn_2^{3+}F(OH)_8]$ framework host, the channel is symmetry constrained and arranged around a 4-fold axis, which does not allow a tetrahedral SO_4 coordination. Attempts failed to describe the extra-framework content with ordered sulfate groups reliably in subgroups of lower symmetry. Data collections of a second crystal as well as a low-temperature measurement revealed no relevant changes of the model although a slight lattice distortion to orthorhombic metrics at 100 K cannot be excluded. As the distance c/2 of ~ 2.8 Å is far too short for neighbouring S atoms belonging to sulfate groups, one can assume the channel to be filled by only 50%, which is in accordance with chemistry and balance of charges required to compensate for the framework $[Ca_2Mn_2^{3+}F(OH)_8]^{1+}$. Minor substitution of Mn^{3+} by divalent ions Cu^{2+}, Mg^{2+} and Ca^{2+} would – as indicated by the chemical analysis – further lead to a reduction of necessary anionic sulfate groups from 0.5 to ~ 0.4 per formula unit. Because of the observed strong disorder, and combined with atomic displacement parameters exhibiting strongly elongated ellipsoids (see Fig. 5) along [001], the formal S–O distances (1.8 Å) of such a simplified model are much too high. Therefore, the hydrogen bonding system can only be estimated. The strongest residual electron density peaks (~ 1.7 and 1.3 e^- $Å^{-3}$) are located on the 4-fold axis within the channel.

From the chemical point of view, saccoite may be classified as 7.BC.65 in the *Strunz Mineralogical Tables* (Strunz and Nickel, 2001), i.e. sulfates with additional anions and without H_2O, with chemical similarities to despujolsite. However, the observed chemistry as an anhydrous Ca, Mn, F bearing sulfate is presently unique. According to its main one-dimensional structural motive saccoite can also be classified as a heterometallic, heteropolyhedral microporous mineral.

Competing interests. The authors declare none.

References

Brese N.E. and O'Keeffe M. (1991) Bond-valence Parameters for Solids. *Acta Crystallographica*, B47, 192–197.

Bruker (2020) *APEX3*. Bruker AXS Inc., Madison, Wisconsin, USA.

Cairncross B., Beukes N.J. and Gutzmer J. (1997) *The Manganese Adventure: The South African Manganese Fields.* Associated Ore & Metal Corporation Limited, South Africa.

Dowty E. (2016) *ATOMS (Version 6.5.0).* Shape Software, Kingsport, Tennessee, USA.

Foster M.D., Rivin I., Treacy M.M.J. and Delgado Friedrichs O. (2006) A geometric solution to the largest-free-sphere problem in zeolite frameworks. *Miocroporous and Mesoporous Materials*, **90**, 32–38.

Giester G. and Rieck B. (1994) Effenbergerite, $BaCu[Si_4O_{10}]$, a new mineral from the Kalahari Manganese Field, South Africa: description and crystal structure. *Mineralogical Magazine*, **58**, 663–670.

Giester G. and Rieck B. (1996) Wesselsite, $SrCu[Si_4O_{10}]$, a further new gillespite-group mineral from the Kalahari Manganese Field, South Africa. *Mineralogical Magazine*, **60**, 795–798.

Giester G., Mikenda W. and Pertlik F. (1996) Kleinite from Terlingua, Brewster County, Texas: investigations by single crystal X-ray diffraction, and vibrational spectroscopy. *Neues Jahrbuch für Mineralogie*, **2**, 49–56.

Giester G., Lengauer C.L., Pristacz H., Rieck B., Topa D. and von Bezing K.-L. (2016) Cairncrossite, a new phyllosilicate from the Wessels Mine, Kalahari Manganese Field, South Africa. *European Journal of Mineralogy*, **28**, 495–505.

Giester G., Lengauer C.L., Topa D., Gutzmer J. and Von Bezing K.-L. (2019) Saccoite, IMA 2019-056. CNMNC Newsletter No. 52. *Mineralogical Magazine*, **83**, https://doi.org/10.1180/mgm.2019.73.

Gladstone J.H. and Dale T.P. (1863) Researches on the refraction, dispersion, and sensitiveness of liquids. *Philosophical Transactions of the Royal Society of London*, **153**, 317–343.

Gnos E., Armbruster T. and Villa I.M. (2003) Norrishite, $K(Mn_2^{3+} Li)Si_4O_{10}(O)_2$, an oxymica associated with sugilite from the Wessels Mine, South Africa: Crystal chemistry and ^{40}Ar–^{39}Ar dating. *American Mineralogist*, **88**, 189–194.

Gunter M.E., Bandli B.R., Bloss F.D., Evans S.H., Su S.-C. and Weaver R. (2004) Results from a McCrone spindle stage short course, a new version of EXCALIBR, and how to build a spindle stage. *The Microscope*, **52**, 23–39.

Gutzmer J. and Beukes N.J. (1993) Fault-controlled metasomatic alteration of early Proterozoic sedimentary manganese ores in the Kalahari manganese field, South Africa. *Economic Geology*, **90**, 823–844.

Gutzmer J. and Beukes N.J. (1996) Mineral paragenesis of the Kalahari manganese field, South Africa. *Ore Geology Reviews*, **11**, 405–428.

Holland T.J.B. and Redfern S.A.T. (1997) Unit cell refinement from powder diffraction data: the use of regression diagnostics. *Mineralogical Magazine*, **61**, 65–77.

Mandarino J.A. (1976) The Gladstone-Dale Relationship – Part I: Derivation of new constants. *The Canadian Mineralogist*, **14**, 498–502.

Mandarino J.A. (1981) The Gladstone-Dale Relationship: Part IV. The compatibility concept and its application. *The Canadian Mineralogist*, **19**, 441–450.

Nasdala L., Akhmadaliev S., Artac A., Chanmuang N. C., Habler G. and Lenz C. (2018) Irradiation effects in monazite-(Ce) and zircon: Raman and photoluminescence study of Au-irradiated FIB foils. *Physics and Chemistry of Minerals*, **45**, 855–871.

Rieck B., Pristacz H. and Giester G. (2015) Colinowensite, $BaCuSi_2O_6$, a new mineral from the Kalahari Manganese Field, South Africa, and new data on wesselsite, $SrCuSi_4O_{10}$. *Mineralogical Magazine*, **79**, 1769–1778.

Sachs A. (1905) Der Kleinit, ein hexagonales Quecksilberoxychlorid von Terlingua in Texas. *Sitzungsberichte der Königlich Preussischen Akademie der Wissenschaften zu Berlin*, **1905**(2), 1091–1094.

Sheldrick G.M. (2015) Crystal structure refinement with SHELXL. *Acta Crystallographica*, **C71**, 3–8.

Sheldrick G.M. (2018) *SHELXL-2018/3*. Universität Göttingen, Göttingen, Germany.

Strunz H. and Nickel E.H. (2001) *Strunz Mineralogical Tables. Chemical-Structural Mineral Classification System.* Ninth Edition, E. Schweizerbart'sche Verlagsbuchhandlung, Stuttgart, Germany, 870 pp.